

The Electrochemical Properties of $\text{Li}_2\text{Ni}_x\text{Mn}_{1-x}\text{SiO}_4$ Cathode Material for Lithium Batteries

Atef Y. Shenouda^{1,*} and N. Munichandraih²

¹Central Metallurgical Research and Development Institute (CMRDI), Tebbin, P.O. Box 87 Helwan, Egypt

²Department of Inorganic and Physical Chemistry, Indian Institute of Science (IISc), Bangalore, India

*E-mail: ayshenouda@yahoo.com

Received: 3 August 2015 / Accepted: 4 August 2016 / Published: 6 September 2016

$\text{Li}_2\text{Ni}_x\text{Mn}_{1-x}\text{SiO}_4$ ($x = 0, 0.2, 0.4, 0.6, 0.8$ and 1) samples were prepared by solid state process. The structure of prepared samples of $\text{Li}_2\text{Ni}_x\text{Mn}_{1-x}\text{SiO}_4$ is characterized by XRD. The crystal structure of the samples is orthorhombic having space group $\text{Pmn}2_1$. SEM investigations are carried out explaining the morphology of powders of these samples. Furthermore, electrochemical impedance spectra measurements are applied. The highest conductivity is achieved with the cell prepared from $\text{Li}_2\text{Ni}_{0.2}\text{Mn}_{0.8}\text{SiO}_4$ compound. Cyclic voltammetric measurements are carried out for $\text{Li}_2\text{Ni}_x\text{Mn}_{1-x}\text{SiO}_4$ material between 0.1 and 4.5 V vs. Li^+ with scan rate 0.1 mVs^{-1} . It is observed that $\text{Li}/\text{Li}_2\text{Ni}_{0.2}\text{Mn}_{0.8}\text{SiO}_4$ cell has initial capacity of 160 mAhg^{-1} . The cycle life performance is carried out for $\text{Li}_2\text{Ni}_x\text{Mn}_{1-x}\text{SiO}_4$ cells. The prepared cells gave average capacities between 100 and 150 mAhg^{-1} .

Keywords: Lithium battery; lithium transition metal silicates.

1. INTRODUCTION

The rechargeable lithium ion batteries (LIB) for portable electronic devices (e.g. PC and laptop computers, wireless and mobile phones, camcorders, .etc.) have lately a strong tendency to expansion [1–6].

Polyanion Li_2MXO_4 , $M = \text{Mn, Fe, Co}$ and Ni and $X = \text{Si, P}$ and S compounds are classified as promising candidates for positive electrode materials in the majority of lithium batteries [7, 8]. These compounds are cheaper and safer than the known uses of lithium transition metal oxides. Thus, different efforts were made to establish other cathode materials for lithium batteries.

Li_2MSiO_4 , $M = \text{Mn, Fe, Co}$ and Ni compounds were prepared and investigated as promising positive materials for lithium ion batteries [9–11]. LiMPO_4 lithium metal phosphate has only one Li^+ ion per structure unit [12–14]. However, Li_2MSiO_4 has 2 Li^+ ions per formula unit, giving a higher

theoretical charge and discharge capacities than phosphates. Therefore, it is considered as a promising alternative positive material for LIB [15–18].

Deng et.al. reported that $\text{Li}_2\text{MnSiO}_4$ is prepared by a $\text{C}_6\text{H}_8\text{O}_7$ acid using sol–gel method [19]. The crystal structure was indexed with orthorhombic unit cell. The $\text{Li}_2\text{MnSiO}_4$ specific discharge capacity was 70 mAh g^{-1} after 20 cycles at current density 1/16 C. The first discharge capacity was retained 37% after fifty cycles. $\text{Li}_2\text{MnSiO}_4$ has small electric conductivity and great irreversibility behavior, which sets to a weak electrochemical behavior.

It was reported that $\text{Li}_2\text{MnSiO}_4$ silicate positive electrode has great charge transfer resistance. This is due to intrinsic poor electronic conductivity. Improvement of orthosilicate cathode can be obtained through doping with another transition metal or composite material [19].

It was reported about the synthesis of a $\text{Li}_2\text{MnSiO}_4/\text{C}$ nanocomposite material through solutions mixture way and solid state reaction process in N_2 atmosphere at 600°C for 10 h. The cell shows a reversible discharge capacity of 209 mAh g^{-1} with a very good rate performance on the contrary of the reported ones for lithium silicate compounds [20].

The aim of this work is to study the different ratios of Ni and Mn in the $\text{Li}_2\text{Ni}_x\text{Mn}_{1-x}\text{SiO}_4$ compound on the electrochemical behaviour and performance of it as positive electrode.

2. EXPERIMENTAL

2.1. $\text{Li}_2\text{Ni}_x\text{Mn}_{1-x}\text{SiO}_4$ samples preparation

$\text{Li}_2\text{Ni}_x\text{Mn}_{1-x}\text{SiO}_4$ ($x = 0, 0.2, 0.4, 0.6, 0.8$ and 1) samples were prepared by solid state process using stoichiometric ratios weights of Li_2CO_3 , $\text{Mn}(\text{CH}_3\text{COO})_2 \cdot 4\text{H}_2\text{O}$, $\text{Ni}(\text{CH}_3\text{COO})_2 \cdot 4\text{H}_2\text{O}$ and SiO_2 . The mixture was ground with a little amount of acetone. In a porcelain crucible the mixture of each sample was heated to 800°C for 12 h in Ar.

2.2. Physical characterization

The crystalline phases were identified by X-ray diffraction (XRD) on a Bruker axis D8 diffractometer with crystallographic data software Topas 2 using Cu-K_α ($\lambda = 1.5406$) radiation operating at 40 kV and 30mA at a rate of $2^\circ/\text{min}$. The particles morphology observed using the scanning electron microscope using JOEL SEM-Model 5040.

2.3. Electrochemical cell assemble and measurements

The working electrode (WE) was prepared from slurry of the 85% active material, 10% C-black and 5% binder (poly vinylidene difluoride: PVDF). The slurry was pasted with some drops of N-methyl pyrrolidone (NMP). Aluminium disk substrate (1 cm^2 area) was coated with this active material to form the WE. The WE was dried in vacuum oven at 100°C . A Teflon cell was used to house the lithium foil metal (Sigma Aldrich) that acts as counter and reference electrode, separator of Celgrad

(micro-porous poly propylene). The electrolyte was 1M LiAsF₆ dissolved in mixture of 1: 1 PC and EC. The cells were assembled inside a glove box MBraun.

Galvanostatic charging and discharging cycling of the cells were achieved with the potentials windows between 1.5 and 4.5 V at total current 0.1 mA using a Bitrode battery tester. Furthermore, impedance measurements were applied using frequency range between 10⁶ and 10⁻² Hz using amplitude of 10 mV using Solartron electrochemical interface model SI 1287.

3. RESULTS AND DISCUSSION

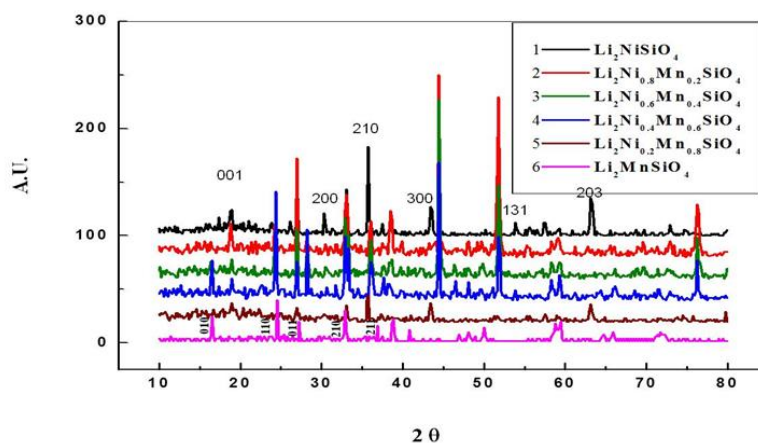
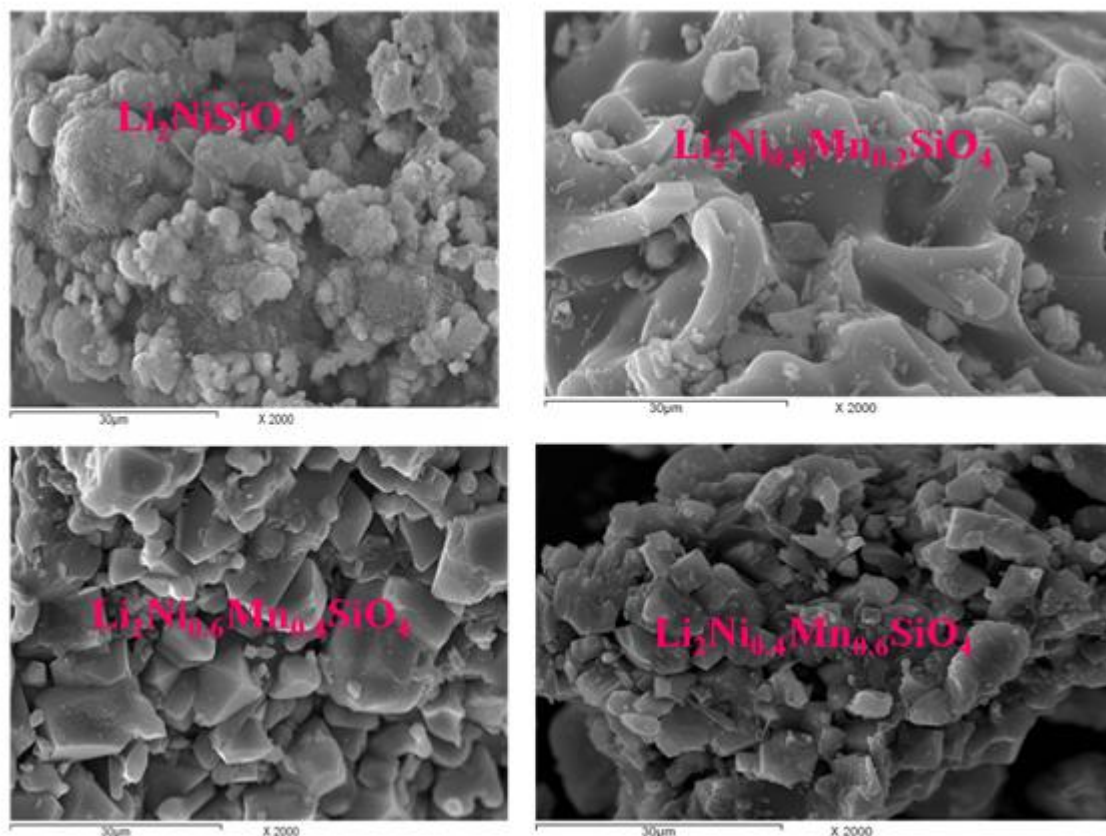


Figure 1. XRD patterns (Cu K_α radiation) of Li₂Ni_xMn_{1-x}SiO₄ (x = 0, 0.2, 0.4, 0.6, 0.8 and 1) samples prepared at 800°C.



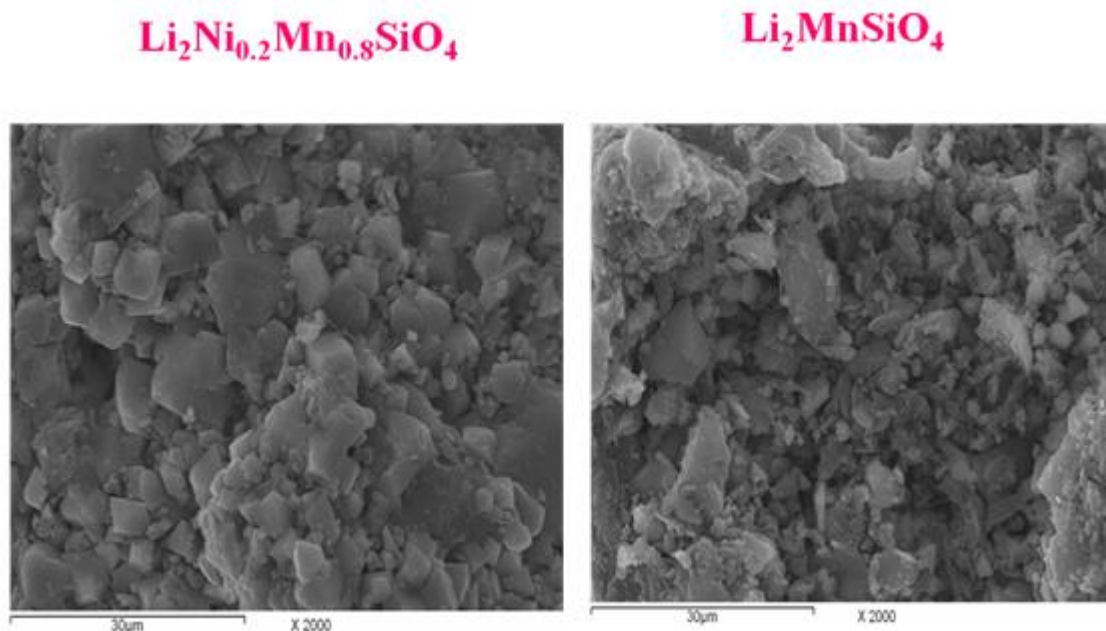
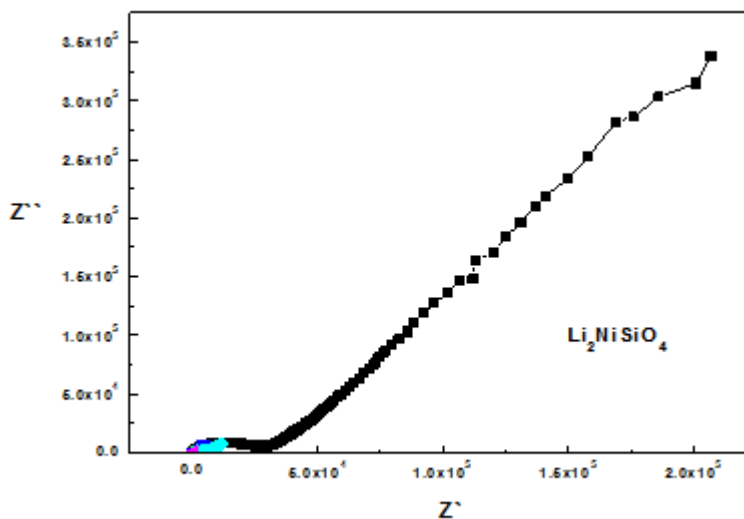


Figure 2. SEM of $\text{Li}_2\text{Ni}_x\text{Mn}_{1-x}\text{SiO}_4$ ($x=0, 0.2, 0.4, 0.6, 0.8$ and 1) samples prepared at

The structure of prepared samples of $\text{Li}_2\text{Ni}_x\text{Mn}_{1-x}\text{SiO}_4$ was characterized by XRD. The patterns are given in Fig.1. XRD patterns of the investigated samples show similar characteristic peaks with samples composition of $x=0.4-1$. Samples can be indexed on the basis of orthorhombic unit cell with space group $\text{Pmn}2_1$ that in agreement with reported ones [21, 22].

SEM morphologies of the samples were investigated as shown in Fig. 2. The morphological structure of materials exhibited aggregated lumps. The average particle sizes of $\text{Li}_2\text{NiSiO}_4$, $\text{Li}_2\text{Ni}_{0.8}\text{Mn}_{0.2}\text{SiO}_4$, $\text{Li}_2\text{Ni}_{0.6}\text{Mn}_{0.4}\text{SiO}_4$, $\text{Li}_2\text{Ni}_{0.4}\text{Mn}_{0.6}\text{SiO}_4$, $\text{Li}_2\text{Ni}_{0.2}\text{Mn}_{0.8}\text{SiO}_4$ and $\text{Li}_2\text{MnSiO}_4$ are 3, 7, 15, 5, 3 and 2 μm , respectively.



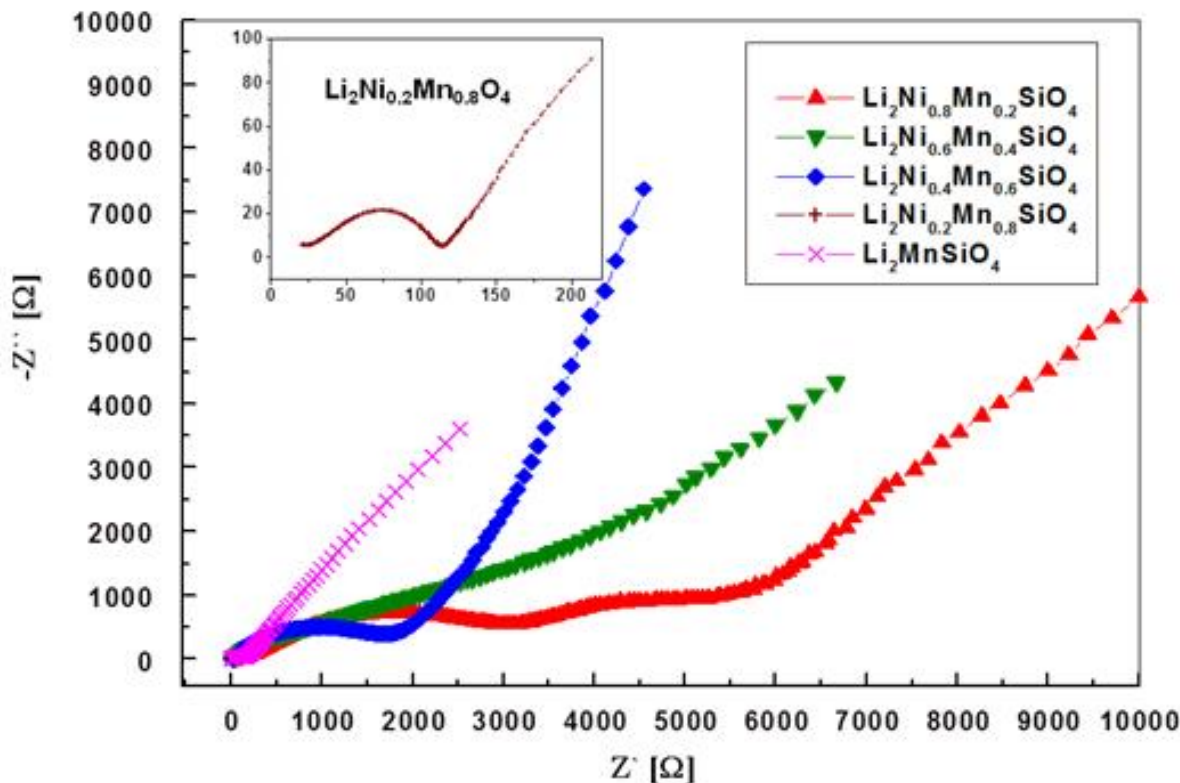


Figure 3. EIS of Li/ Li₂Ni_xMn_{1-x}SiO₄ (x= 0, 0.2, 0.4, 0.6, 0.8 and 1) cells.

The electrochemical impedance spectra (EIS) of the cells as illustrated in Fig.3 show an intercept at high frequency for the resistance of the electrolyte, R_e on the real axis Z' , followed by a semicircle in the high-middle frequency region, and a straight line in the low frequency region. The numerical value of the diameter of the semicircle on the Z'_{re} axis is approximately equal to the charge transfer resistance, R_{ct} . It is observed that Li_2MnSiO_4 and Li_2NiSiO_4 cells have high R_{ct} in comparison with the other cells. In fact, electrochemical impedance spectroscopy (EIS) may be considered as one of the most sensitive tools for the study of differences in the electrode behavior due to surface modification. It is observed that the cell prepared from $Li_2Ni_{0.2}Mn_{0.8}SiO_4$ has the lowest real Z'_{re} (charge transfer resistance: 114 Ω) in comparison with the other cells.

The relation between Z'_{re} and the inverse of the square root of the lower angular frequencies ($\omega^{0.5}$) is given in Fig.4. The straight lines are attributed to the diffusion of the lithium ions inside the bulk of the electrode materials. This is called Warburg diffusion [5, 23, 24]. This relation is governed by Equations 1 and 2.

$$Z_{re} = R_e + R_{ct} + \sigma_w \cdot \omega^{-0.5} \tag{1}$$

$$D = 0.5 (RT / A n^2 F^2 \sigma_w C)^2 \tag{2}$$

Where ω : angular frequency in the low frequency region, D : diffusion coefficient, R : the gas constant, T : the absolute temperature, F : Faraday's constant, A : the area of the electrode surface, and C : molar concentration of Li^+ ions. Furthermore, the exchange current density ($i^0 = RT/nFR_{ct}$). It is observed that the Warburg impedance coefficient (σ_w) is 41.5 $\Omega \cdot s^{-0.5}$ for $Li_2Ni_{0.2}Mn_{0.8}SiO_4$ cell and this

is the lowest value in comparison with those of the other samples. The impedance parameters of the samples are recorded in Table.1.

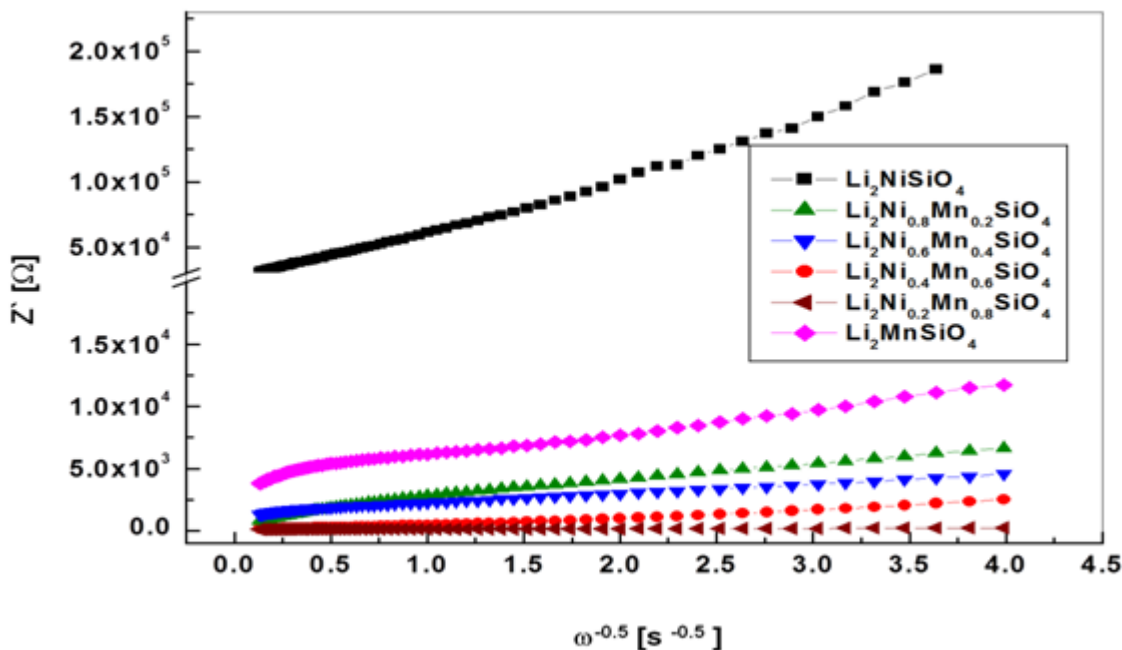


Figure 4. Relationship between real impedance with the low angular frequencies for Li/ Li₂Ni_xMn_{1-x}SiO₄ (x= 0, 0.2, 0.4, 0.6, 0.8 and 1) cells.

Table 1. Electrochemical Impedance parameters of Li/Li₂Ni_xMn_{1-x}SiO₄ (x= 0, 0.2, 0.4, 0.6, 0.8 and 1) cells.

sample	R _{ct} [Ω]	σ _w [Ω.s ^{0.5}]	D [cm ² /s]	i ^o [mAcm ⁻²]	C _{dl} [F]
Li ₂ NiSiO ₄	31252	46802.96	1.62E-17	8.24E-07	5.09E-09
Li ₂ Ni _{0.8} Mn _{0.2} SiO ₄	5740	1809.599	1.08E-14	4.69E-06	1.60E-08
Li ₂ Ni _{0.6} Mn _{0.4} SiO ₄	3499	1382.293	1.85E-14	7.39E-06	7.90E-07
Li ₂ Ni _{0.4} Mn _{0.6} SiO ₄	1954	757.1065	6.18E-14	1.32E-05	2.96E-07
Li ₂ Ni _{0.2} Mn _{0.8} SiO ₄	113.86	37.28176	2.55E-11	2.35E-04	4.63E-06
Li ₂ MnSiO ₄	264	639.2388	8.66E-14	1.06E-04	2.63E-06

It is observed that the charge transfer resistance of Li₂Ni_{0.2}Mn_{0.8}SiO₄ cell is the lowest one in comparison with the other cells. F. Wang et al. reported that R_{ct} was 1611 Ω for Li₂MnSiO₄/ Li cell [24]. Thus, the obtained result is better (264 Ω) than the reported one.

The first charge and discharge capacity plateaus vs. the working voltage between 4.5 and 1.5V are shown in Fig.5. The maximum first discharge specific capacity, 164 mAh g⁻¹ is obtained with the Li₂Ni_{0.2}Mn_{0.8}SiO₄ cell. Fig. 6 illustrates the specific discharge cyclic performance of the different cells. It is clearly observed that the reversible specific discharge capacity has achieved until 100 cycles. The average specific discharge capacity is about 150 mAhg⁻¹.

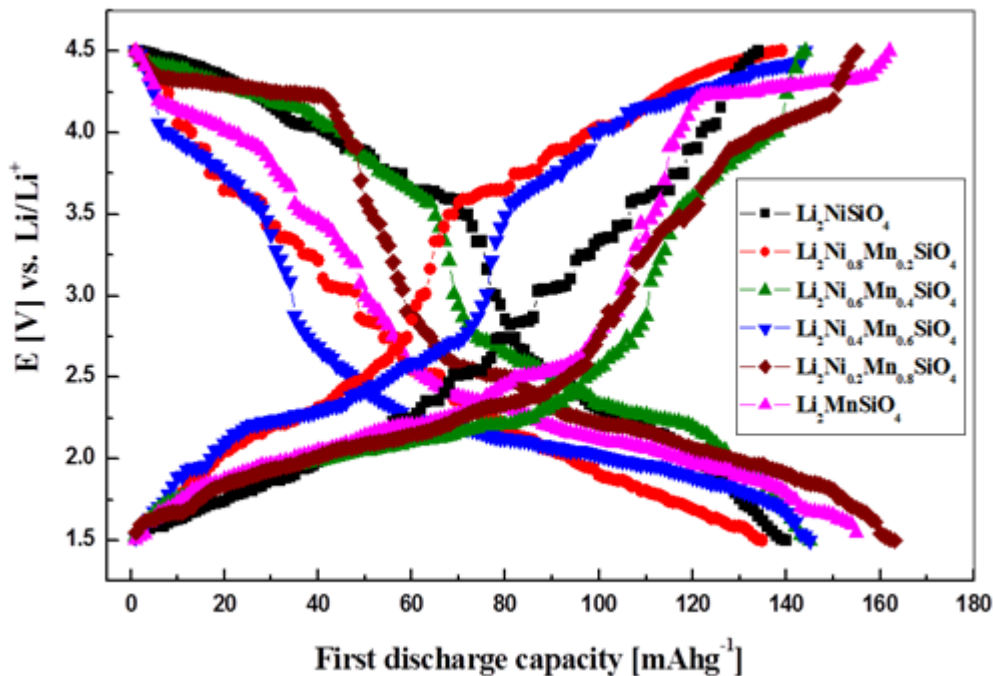


Figure 5. Voltage- capacity profiles for Li / $\text{Li}_2\text{Ni}_x\text{Mn}_{1-x}\text{SiO}_4$ ($x=0, 0.2, 0.4, 0.6, 0.8$ and 1) cells.

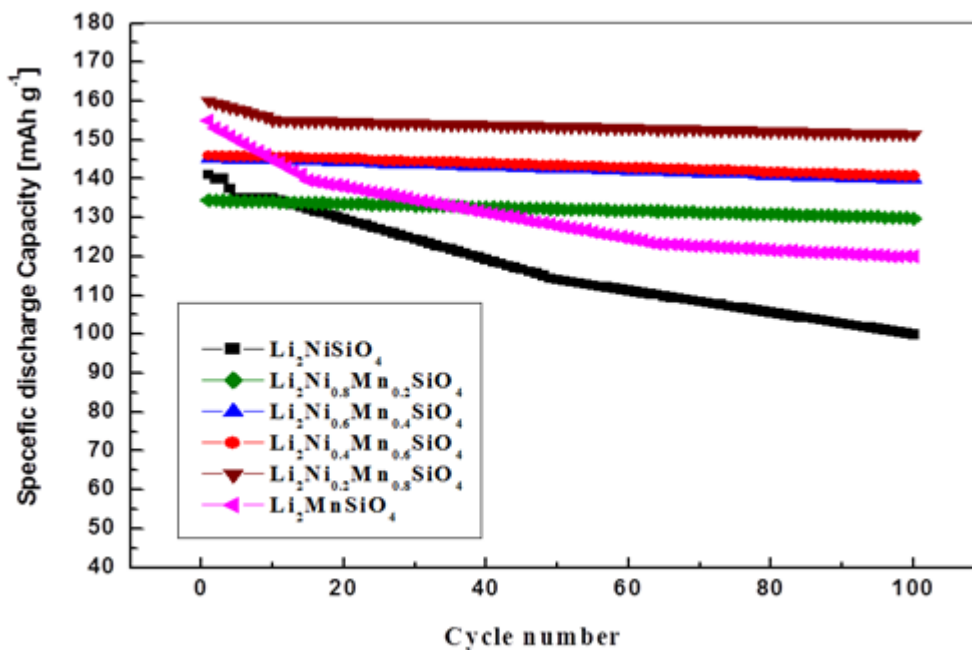


Figure 6. Cycle life performance of Li / $\text{Li}_2\text{Ni}_x\text{Mn}_{1-x}\text{SiO}_4$ ($x=0, 0.2, 0.4, 0.6, 0.8$ and 1) cells.

The cell prepared from $\text{Li}_2\text{Ni}_{0.2}\text{Mn}_{0.8}\text{SiO}_4$ sample shows maximum discharge capacity, 155 mAhg^{-1} . Cycling performance of the $\text{Li}_2\text{Ni}_{0.2}\text{Mn}_{0.8}\text{SiO}_4$ has been improved with mild manganese substitution while decreased with heavy manganese substitution. It was reported about the cycle performance of $\text{Li}_2\text{MnSiO}_4$ that it decreased to $60\text{-}70 \text{ mAhg}^{-1}$ after 50 cycles [19, 25]

4. CONCLUSION

The structure of prepared samples of $\text{Li}_2\text{Ni}_x\text{Mn}_{1-x}\text{SiO}_4$ was characterized by XRD using. Samples are matched with the data of orthorhombic unit cell with space group $\text{Pmn}2_1$. The morphological structure of materials exhibited aggregated lumps. The average particle sizes of $\text{Li}_2\text{NiSiO}_4$, $\text{Li}_2\text{Ni}_{0.8}\text{Mn}_{0.2}\text{SiO}_4$, $\text{Li}_2\text{Ni}_{0.6}\text{Mn}_{0.4}\text{SiO}_4$, $\text{Li}_2\text{Ni}_{0.4}\text{Mn}_{0.6}\text{SiO}_4$, $\text{Li}_2\text{Ni}_{0.2}\text{Mn}_{0.8}\text{SiO}_4$ and $\text{Li}_2\text{MnSiO}_4$ are 3, 7, 15, 5, 3 and 2 μm , respectively. It is observed that the cell prepared from $\text{Li}_2\text{Ni}_{0.2}\text{Mn}_{0.8}\text{SiO}_4$ has the lowest real Z_{re} (charge transfer resistance: 113.86 Ω) in comparison with the other cells. It is observed that the Warburg impedance coefficient (σ_w) is 41.5 $\Omega \cdot \text{s}^{-0.5}$ for $\text{Li}_2\text{Ni}_{0.2}\text{Mn}_{0.8}\text{SiO}_4$ cell and this is the lowest value in comparison with those of the other samples. Also, this cell has max. diffusion coefficient, $2.55 \times 10^{-11} \text{cm}^2 \text{s}^{-1}$. The cell prepared from $\text{Li}_2\text{Ni}_{0.2}\text{Mn}_{0.8}\text{SiO}_4$ sample shows maximum discharge capacity, 155 mAhg^{-1} . Cycling performance of the $\text{Li}_2\text{Ni}_{0.2}\text{Mn}_{0.8}\text{SiO}_4$ has been improved with mild manganese substitution while decreased with heavy manganese substitution.

ACKNOWLEDGEMENT

Dr. Atef Shenouda would like to offer his thanks to Federation of Indian Chambers of Commerce and Industry (FICCI) for awarding him the visiting fellowship program to conduct some of this research in IISc.

References

1. A. Y. Shenouda, *Electrochim. Acta*, 51 (2006) 5973.
2. A. Y. Shenouda and K.R. Murali, *J. Power Sources*, 176 (2008) 332.
3. A. Y. Shenouda and Hua Kun Liu, *J. Power Sources*, 185 (2008) 1386 - 1391.
4. A. Y. Shenouda, Hua K. Liu, *J. Alloys and Comp.*, 477 (2009) 498.
5. A. Y. Shenouda, Hua K. Liu, *J. Electrochem. Soc.*, 157 (2010) A 1183.
6. A. Y. Shenouda El Sayed M. El Sayed and Hua Kun Liu, *J. New Materials for Electrochemical Systems* 14 (2011) 19.
7. L. Shi, W. Xie, Q. Ge, S. Wang, D. Chen, L. Qin, M. Fan, L. Bai, Z. Chen, H. Shen, G. Tian, C. Lv, K. Shu, *Int. J. Electrochem. Sci.*, 10 (2015) 4696.
8. C. Wei, J. Deng, L. Xi, H. Zhou, Z. Wang, C.Y. Chung, Q. Yao, G. Rao, *Int. J. Electrochem. Sci.*, 8 (2013) 6775.
9. A.K. Padhi, K.S. Nanjundaswamy, C. Masquelier, S. Okada, J.B. Goodenough, *J. Electrochem. Soc.* 144 (1997) 1609- 1613.
10. A. Nyten, A. Abouimrane, M. Armand, T. Gustafsson, J.O. Thomas, *Electrochem. Commun.* 7(2005) 156- 160.
11. K. Zaghbi, A. Ait Salah, N. Ravet, A. Mauger, F. Gendron, C.M. Julien, *J. Power Sour.* 160 (2006) 1381.
12. A. Nyten, S. Kamali, L. Hangstrom, T. Gustafsson, J.O. Thomas, *J. Mater. Chem.* 16 (2006) 2266.
13. A.Y. Shenouda, H.K. Liu, *J. Alloys Compd.* 477 (2009) 498.
14. Y. Liu, C.H. Mi, C.Z. Yuan, X.G. Zhang, *J. Electroanal. Chem.* 628 (2009) 73.
15. H. Huang, S.C. Yin, L.F. Nazar, *Electrochem. Solid-State Lett.* 4 (2004) A170.
16. M. Armand, C. Michot, N. Ravet, M. Simoneau, P. Hovington, US patent 6085015 (2000).
17. S. Zhang, C. Deng, S.Y. Yang, *Electrochem. Solid-State Lett.* 12 (2009) A136.
18. R. Dominko, M. Bele, M. Gaberscek, M. Remskar, D. Hanzel, S. Pejovnik, J. Jamnik, *J. Power Sources* 153 (2006) 274–280.
19. C. Denga, S. Zhang, B.L. Fu, S.Y. Yang, L. Ma, *Mater. Chem. and Phys.* 120 (2010) 14–17.

20. Yi-Xiao Li, Zheng-Liang Gong, Yong Yang *J. Power Sources* 174 (2007) 528–532.
21. A.S. Prakash, P. Rozier, L. Dupont, H. Vezin, F. Sauvage, J.M. Tarascon, *Chem. Mater.* 18 (2006) 407.
22. R.J. Gummow and Y. He, *J. Power Sources* 253 (2014) 315-331.
23. X. Huang, X. Li, H. Wang, Z. Pan, M. Qu, Z. Yu, *Solid State Ionics* 181 (2010) 1451–1455.
24. F. Wang, J. Chen, C. Wang, B. Yi, *J. Electroanal Chem.* 688 (2013) 123–129.
25. C. Deng, S. Zhang, B.L. Fu, S.Y. Yang, L. Ma, *Mater. Chem. and Phys.* 120 (2010) 14–17.

© 2016 The Authors. Published by ESG (www.electrochemsci.org). This article is an open access article distributed under the terms and conditions of the Creative Commons Attribution license (<http://creativecommons.org/licenses/by/4.0/>).